Manufacturing Scale-Up of Anodeless Solid State Lithium Thin Film Battery for High Volumetric Energy Density Applications

Diyi Cheng[1], Khanh Tran[2], Shoba Rao[2], Zhongchun Wang[2], Richard van der Linde[2], Shahid Pirzada[2], Hui Yang[2], Alex Yan[2], Arvind Kamath[2,*] and Ying Shirley Meng[1,3,*]

[1]*Materials Science and Engineering Program, University of California San Diego, La Jolla, CA, 92093, USA.*

[2]*Ensurge Micropower, San Jose, CA, 95134, USA.*

[3]*Pritzker school of Molecular Engineering, University of Chicago, Chicago, IL, 60637, USA*

* Co-correspondence: arvind.kamath@ensurge.com, shirleymeng@uchicago.edu

Abstract:

Compact, rechargeable batteries in the capacity range of 1-100 mAh are targeted at form-factor-constrained wearables and other high-performance electronic devices, which have core requirements including high volumetric energy density (VED), fast charging, safety, surface-mount technology (SMT) compatibility and long cycle life. Solid-state lithium thin film batteries (TFB) fabricated on thin substrates and packaged in a multilayer stack offer these attributes, overcoming the limitations of lithium-ion batteries based on liquid electrolytes. To maximize the VED, an anodeless architecture fabricated using a roll-to-roll process on an ultrathin stainless-steel substrate (10-75 μm in thickness) has been developed. These microbatteries use a lithium cobalt oxide ($LiCoO_2$) cathode and lithium phosphorus oxynitride (LiPON) electrolyte deposited by thin film techniques to enable key battery performance metrics. A high-device-density dry-process patterning flow defines customizable battery device dimensions while generating negligible waste.

The entire fabrication operation is performed in a conventional, humidity-controlled cleanroom eliminating the need for a costly dry-room environment that allows for simplified, lower-cost manufacturing. Such scale-up using an anodeless architecture also enables a thermal-budget-compatible packaging and metallization scheme targeted at industry-compatible SMT processes. Further manufacturability improvements such as the use of high-speed tests add to the overall range of elements necessary for mass production. A perspective on requirements and opportunities for this technology as it evolves is provided.

Table of Contents Graphic

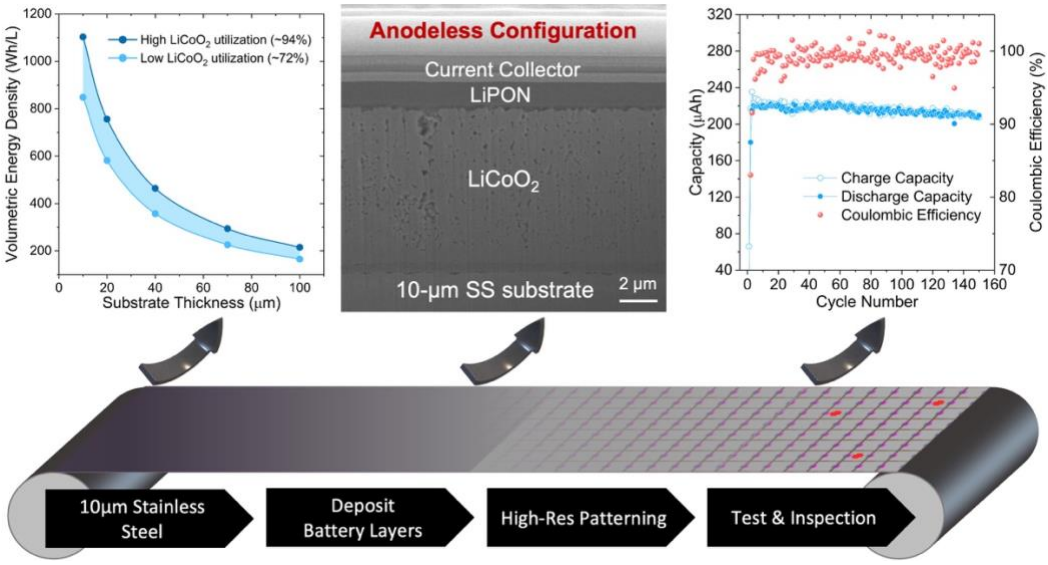

Main text

Lithium battery technology has undergone rapid development in the past decades since the discovery of layered oxide cathode material in the 1970s, and now serves as power sources for various applications that range from portable device to electric vehicles and stationary energy storage systems.[1–3] In the present lithium battery catalogue, all-solid-state battery (ASSB) provides improved safety and energy density over the liquid electrolyte counterparts, which therefore has garnered increased attention and research efforts in the past years.[4,5] Sharing a similar formulation concept, solid-state lithium thin film battery (TFB) is one of the ASSBs that utilizes solid-state electrolyte and active electrode thin films produced via vacuum deposition techniques such as sputtering, atomic layer deposition, etc. TFB was pioneered by Oak Ridge National Laboratory in 1992,[6,7] where J. B. Bates et al. produced a thin film solid-state electrolyte (SSE) named lithium phosphorus oxynitride (LiPON) by substituting 5%-8% of O with N in Li_3PO_4 via radio-frequency (RF) sputtering in nitrogen atmosphere.[6]

LiPON then rapidly drew research attention in the ASSB field. On one hand, TFB typically consists of layered architecture with well-defined interface cell geometry, which serves as an ideal platform for fundamental research on interfaces and electrochemical behaviors within the system;[8,9] More importantly, LiPON exhibits exemplary cyclability with a vast choices of electrode materials, i.e., $LiCoO_2$,[10] $LiMn_2O_4$,[10] $LiNi_{0.5}Mn_{1.5}O_4$,[11] $Li_4Ti_5O_{12}$,[12] Si,[13,14] and Li metal,[10–12] etc. TFBs employing lithium phosphorus oxynitride (LiPON) solid electrolyte have demonstrated remarkable high-voltage compatibility (up to 5V) and high capacity retention over thousands of cycles with low rates of self-discharge.[11,15]

Given the promise of LiPON material in battery applications, many sensed the opportunity of commercializing LiPON-based TFBs. Right after the birth of LiPON, the first TFB patent was

issued in 1994 and was commercially licensed.[16] In the following years, several others joined the effort of LiPON commercialization.[17,18] Although the market has seen promising LiPON-based products during the rapid-development timeframe, the products remained confined to niche applications.[19,20] Key limitations include the following: The thin nature of cathode material in TFB and single-layer cell configuration determines that the energy stored in such limited devices is suited mainly for small-capacity applications. In addition, the small area form factors primarily used thick, rigid substrates (e.g. silicon or glass) that largely limit the versatility and VED of the resulting cells.

Meanwhile, other research efforts have attempted to increase the yield of LiPON synthesis in order to make it compatible with bulk-scale ASSB. Muñoz et al. obtained LiPON glass via ammonolysis in a tube furnace after heat treatment from 600 °C to 750 °C. However, the ionic conductivity of LiPON glass was compromised by two to four orders of magnitude compared with its thin-film analogue.[21] Alternative methods such as plasma-torch-assisted synthesis[22] and ball milling[23] were able to produce LiPON in large batches, but these processes have also generated issues like high interfacial impedance between particles or altered LiPON properties.

Fresh attention was placed on LiPON with the comeback of Li metal anode in the battery field around late 2010s.[24–32] Due to the superior electrochemical stability of LiPON against Li metal anode shown by Dudney et al. in 2015,[11] LiPON has great potential to enable Li metal batteries as either SSE or protective coating layer. Fresh insights gained on the interfacial chemistry between Li metal and LiPON also shed light on interface engineering in bulk Li metal batteries.[9,33,34] LiPON-based TFBs gained popularity with an anodeless configuration that could largely increase the cell energy density.

Concurrently, the miniaturization of electronics has been a trending direction due to the advancement in wearable, hearable and implantable technologies. Compact electrochemical energy storage components that can be integrated to power the electronic system for the life of the device are increasingly needed at commercial scale.[35] LiPON-based TFBs serve as a solution as they offer significantly higher energy density and provide form factor flexibility due to its modifiable cell dimensions. However, the current TFB market requires technology and manufacturing breakthroughs at large scale to meet a higher volumetric energy density (VED). Most commercial batteries using thin film technology have been restricted to low capacity, low VED niche applications primarily due to the substrate choice. Common substrate materials for TFB fabrication include alumina, silicon, sapphire, mica etc. which are typically thick, rigid, electrically insulating, brittle and expensive. These features lead to low VED, limited area form factor that limits such TFBs to niche applications with capacities in the range around 250 μAh, unsuitable for mAh-class applications.

Figure 1A plots the VED of TFB with various cell configuration and materials (Detailed parameters used for calculation listed in **Table S1**). In depicted three cases, lithium (Li) metal serves as anode material since it provides the highest capacity and high cell voltage; LiPON serves as solid-state electrolyte, for its excellent stability and cyclability against varying electrode materials; Lithium cobalt oxide ($LiCoO_2$) is chosen as cathode material because of its fairly high electrode potential against Li anode, high capacity and good cycling stability. For lab-scale development, $LiCoO_2$ thickness is usually targeted around 4 μm and common material such as alumina (Al_2O_3) is used as substrate, which combined gives relatively low VED due to the low cathode loading and high substrate volume.[15] In some commercially available TFB products, cathode thickness is targeted at 7-10 μm.[36] Nevertheless, due to the use of mica-based substrate

that is over tens of microns thick, cell VED is limited to below 200 Wh/L, not to mention the additional wasted volume on packaging materials. To boost the VED significantly, two approaches are key.

The first is to employ an anodeless configuration, where a Li metal anode is not deposited during cell fabrication but instead formed in situ during the first charge cycle. Several merits come with this approach. No Li metal deposition is needed during manufacturing, which simplifies the manufacturing environment and process flow, avoiding potential air exposure during subsequent operations. The absence of Li metal anode enables reflow soldering process while attaching onto PCBs (printed circuit boards) as the typical temperature of reflow soldering (235 °C) leads to Li metal melting.[35] As there is no extra lithium source, anodeless TFB does not have the concern of over discharging during battery operation that can cause irreversible cathode material degradation.[15]

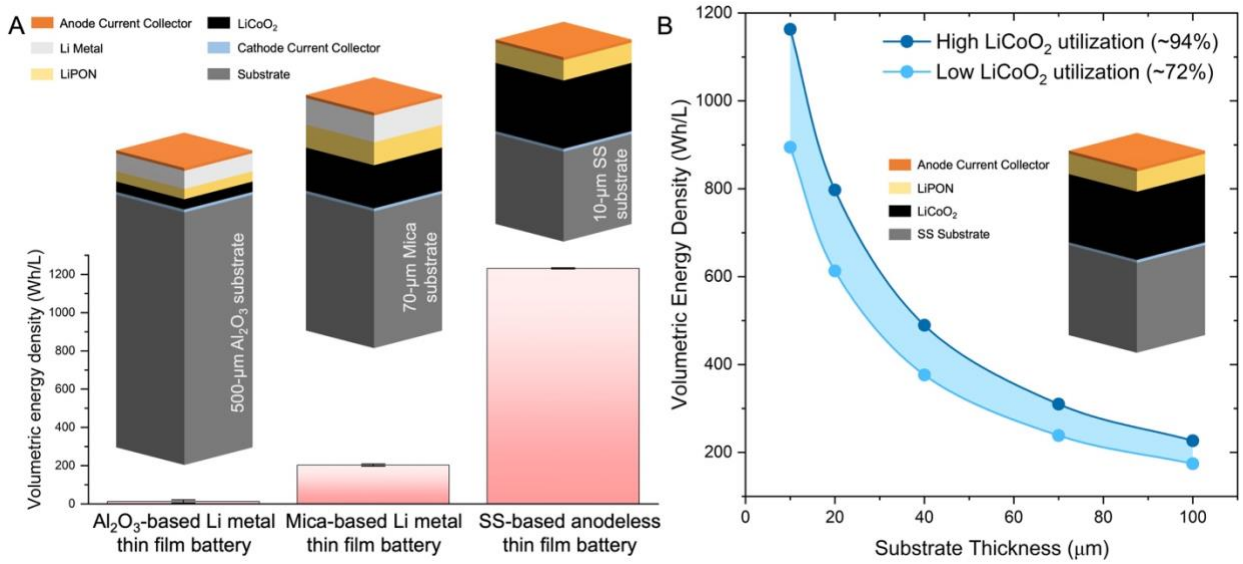

Figure 1. (A) Schematics of Li metal thin film batteries with different cell architectures and corresponding VEDs. (B) VEDs of SS-based anodeless thin film battery with varying SS thicknesses

The second component for boosting VED is to use an ultrathin substrate and reduce the packaging material volume to minimize the inactive volumetric component at the product level.

Note that a high utilization of thin film cathode capacity requires high temperature annealing of the cathode during or post deposition.[37] Therefore, a thin, high-temperature-compatible and low-cost substrate is needed, such as stainless steel (SS). As such, the third cell configuration in **Figure 1A** employs an anodeless approach on a thin SS substrate (10-μm thick), which can yield an unpackaged VED up to 1232 Wh/L when a 10-μm-thick $LiCoO_2$ is used. Thin SS substrate is not only crucial for improving VED, but also bringing merits for manufacturing as it is electrically conductive, flexible and less costly than the substrates typically used for TFB manufacture. **Figure 1B** further demonstrates the impact of substrate thickness on the VED of TFB. As SS substrate thickness increases from 10 μm to 100 μm, the corresponding entitlement VEDs drops from 1163 Wh/L to 227 Wh/L when the cathode utilization is around 94%, emphasizing the essence of utilizing thin substrates with high cathode utilization efficiency.

As such, we demonstrate a successful employment of anodeless configuration in TFB where a thin SS substrate is used. The combination of thick LCO cathode (10 μm in thickness) and thin substrate are able to deliver a much-improved VED. Beyond the battery performance, a roll-to-roll deposition strategy and single-step patterning process are applied which greatly increases the manufacturability on thin substrates. The operation is performed in a standard clean room under normal humidity control without any wet chemical used or generated, further reducing the production cost while minimizing waste and environmental impact. Subsequent high-speed parallel cell parametric electrical measurement is employed to quantify battery characteristics prior to subsequent cell stacking operations. Such products have great potential for the market applications of the internet of things (IoT), hearables and wearables where the need for battery capacity is in the range of 1-100 mAh which are form-factor and space constrained.

In typical TFB fabrication, as most of the substrates are made of rigid, thick materials, a roll-to-roll manufacturing process is not feasible. For ultrathin and flexible substrates, a manufacturing flow was developed as depicted in **Figure 2**. **Figure 2A** shows the general procedure for efficient TFB manufacturing. After deposition, high-resolution patterning is applied to define and isolate the individual cells from each other, which subsequently goes through battery parametric measurements and inspection. With deposition and annealing parameters well-tuned, such roll-to-roll process produces high-quality LCO cathode as shown in **Figure 2B**. Cross-section examination by focused ion beam scanning electron microscopy (FIB/SEM) in **Figure 2C** illustrates a dense 10-μm-thick LCO cathode film with minimal number of voids observed. The LCO cathode film further manifests a preferred (012)-crystal-orientation based on X-ray diffraction (XRD) result in **Figure 2D**, which facilitates lithium-ion transport at cathode-electrolyte interface. **Figure 2E** shows the subsequent workflow after the impedance inspection, where cells are singulated from the sheet and go through a stacking process including encapsulation and metallization to form the final product. Owing to the anodeless nature of such TFB, cell handling after singulation takes place in normal cleanroom environment, with no dry room needed, which further brings down the production cost.

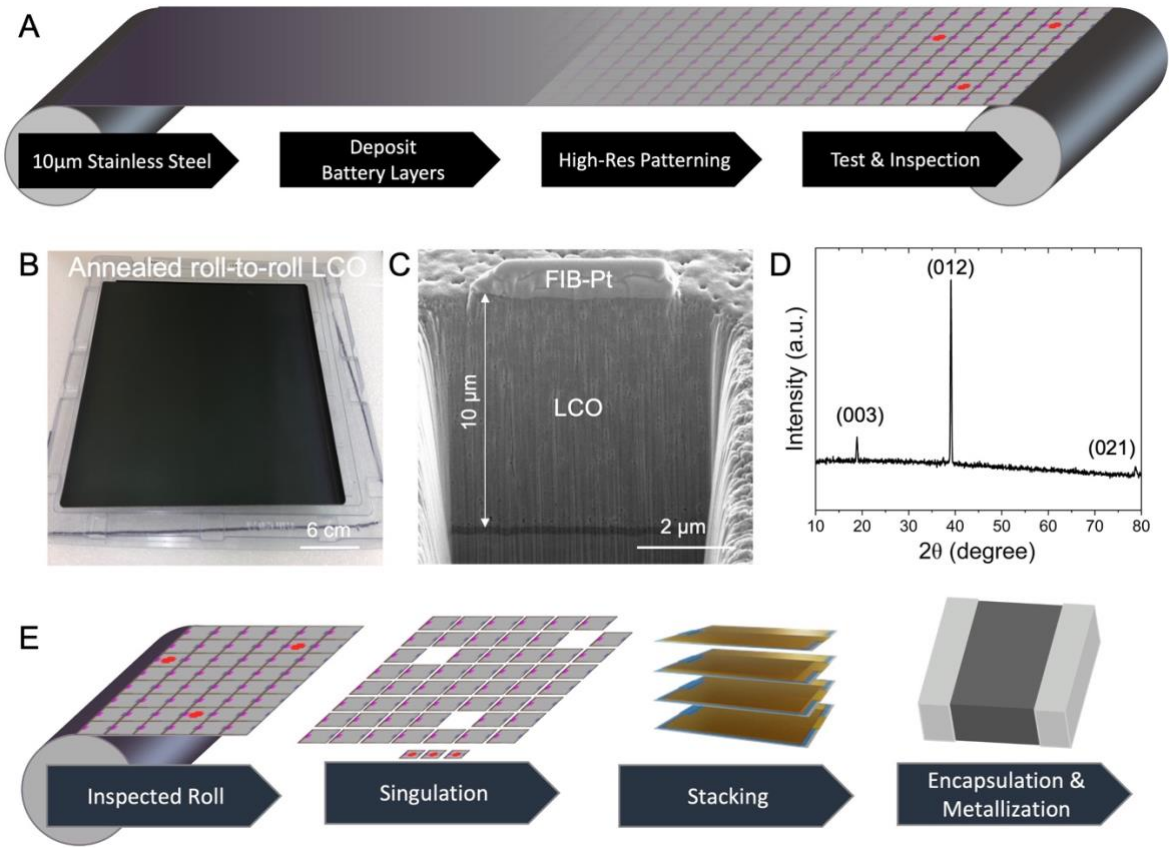

Figure 2. (A) Schematic of the high-throughput roll-to-roll deposition. (B) Photo of an annealed roll-to-roll LCO sheet. (C) Cross-section FIB/SEM image of annealed roll-to-roll LCO. (D) XRD result collected on LCO sheet. (E) Schematic of the dry-process manufacturing flow.

The schematic in **Figure 3A** illustrates the high-resolution patterning process required for high-throughput production. The battery sheet after deposition is patterned, resulting in electrical isolation of each cell with defined dimensions. Unlike previously reported procedures where wet acidic and basic chemicals are typically used for pattering purpose,[35] the patterning process developed in this work is performed under dry conditions. **Figure 3B** displays a photo of singulated patterned cells. The cells show uniform dimensions as targeted by the patterning process. Based on the dimensional footprint requirements, such a patterning process can accurately tune the form factors of the final product. The passing single cell units are assembled to build stacked multilayers as shown in **Figure 3C**. Stacked cells connected in parallel share the same pair of terminals for

electrochemical cycling while isolated from each other by insulating packaging films between each layer. Such a packaging process is the enabler for producing stacked cells (**Figure 3D**) with various capacity ranges to meet different application needs. Due to the adjustable dimensions of the single cell base unit, the stacked cell can fit in a variety of product dimensions as required.

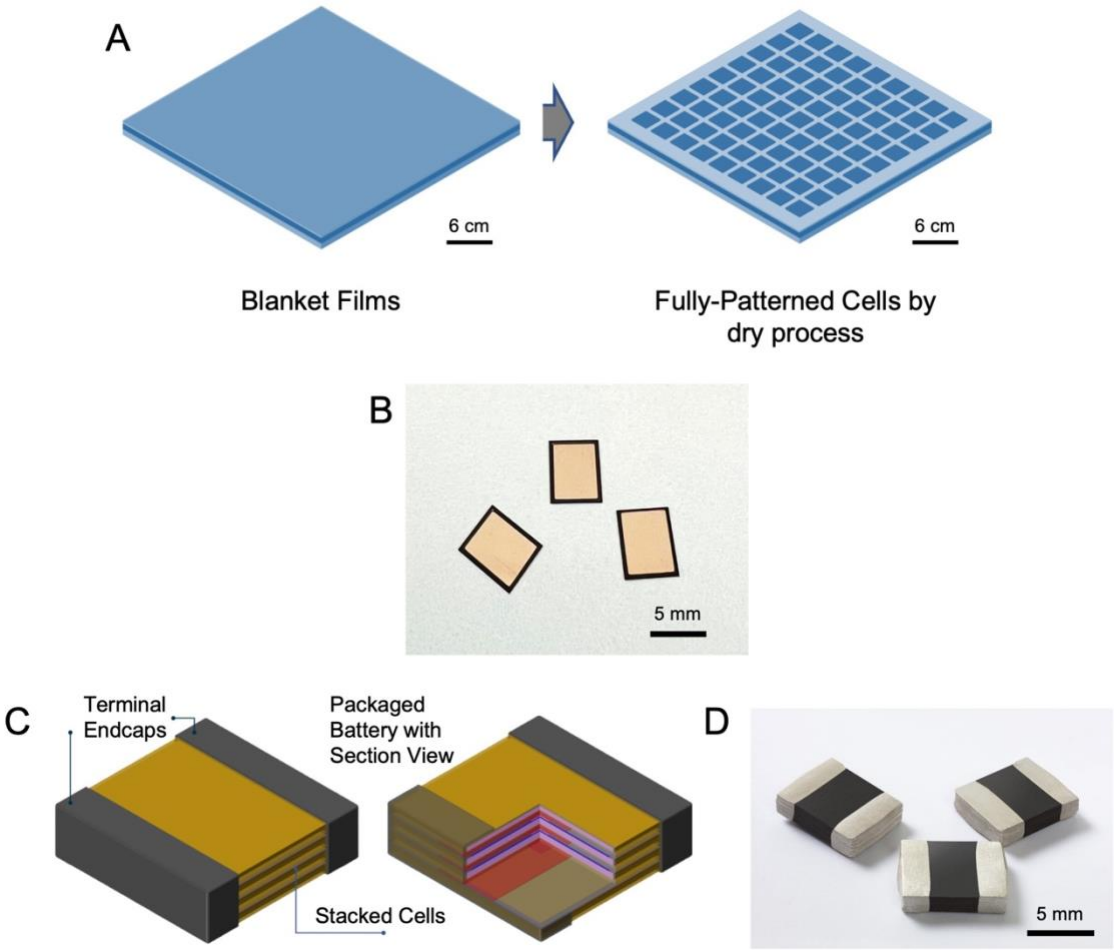

Figure 3. (A) Schematic of the dry-process cell patterning and singulation. (B) Photo of the singulated cells. (C) Schematic of the stacked cells with cross-section view. (D) Photo of the stack cells.

Along with the mass production of singulated cells, a production-grade electrochemical test methodology is needed for high-speed parallel-site testing. A customized roll-to-roll compatible test setup is used to perform electrochemical measurements including open-circuit voltage (OCV) and electrochemical impedance spectroscopy (EIS), etc. at the sheet level. After measurement, the

OCV or impedance values are extracted and plotted in accordance with the physical location of individual cells to form a heat map as the OCV mapping illustrates in **Figure 4A**. Based on the OCV and impedance values, single cells are binned (similar to semiconductor testing), in order to predict battery performance and quality. **Figure 4B** displays a typical EIS curve of a single cell, showing a low cell impedance. The singulated cell can be then transferred to a battery cycler for electrochemical sample testing. **Figure 4C** demonstrates the cycling performance example of a singulated cell. The capacity retention is able to reach approximately 95% after 150 cycles. As shown in **Figure 4D**, the singulated and multilayer stacks are cycled with an industry-compatible potentiostatic charging and a galvanostatic discharging step. By multilayer stacking, the accessible discharge capacity achieves mAh capacity with all the layers connected in parallel and functional. The test methodology classifies the quality of singulated cells in large batches with EIS-based process control.

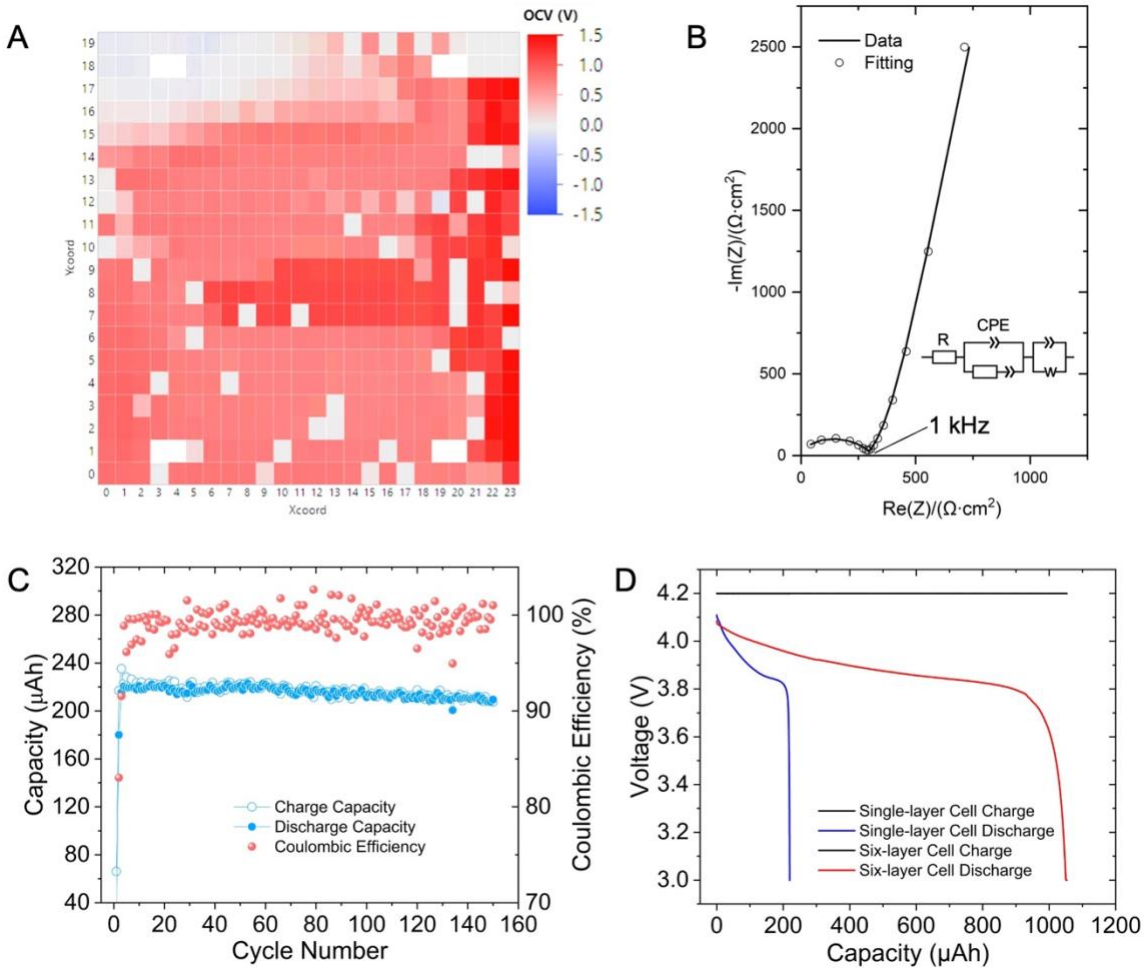

Figure 4. (A) Open-circuit voltage heat map generated based on high-throughput electrochemical measurement. (B) EIS plot of a full cell showing the low cell impedance. (C) Cycling performance of anodeless full cell. D) Voltage curves of the single-layer cell and multi-layer mAh-class cell.

Conclusions and Outlook

In summary, a manufacturing process flow that incorporates roll-to-roll production on ultrathin stainless steel in a dry-process manufacturing is demonstrated with an anodeless cell architecture. Customized form factors with ultrathin packaging deliver industry-leading electrochemical performance and VED for space-constrained product formats. Methodologies such as high-throughput patterning, high-speed electrochemical testing and multilayer stacked

packaging are critical towards commercializing high-VED TFB with considerably flexible form factors and long cycle life.

To this end, several aspects can be considered for future development of high-VED TFB. First, as VED is expected to see a large increase with thinner substrates, exploring new options of suitable substrates and reduced substrate thickness are potential ways to further boost the VED of TFB, in addition to reducing thickness of inactive packaging materials. The second aspect is to produce TFB with higher cell capacity by increased cathode thickness and using higher-capacity cathode materials, both of which are challenging especially when the cycle life needs to be on par with currently available 10-µm LCO cathode. The use of flexible 10-µm-thick stainless-steel substrates offers tremendous new options to product designers in the form of curved and bendable shapes that are mechanically robust. As this technology combines microelectronics manufacturing with battery chemistry, the needs for higher throughput deposition techniques, low defectivity of source materials, high-speed inspection, and test methodology grant rich opportunities for industry and academia to collaborate and enable entirely new generations of end products.

Acknowledgements

D.C. is grateful for the internship training and funding support during that period by Ensurge Micropower. Y.S.M. gratefully acknowledges the partial funding support for interface characterization from the U.S. Department of Energy, Office of Basic Energy Sciences, under Award Number DE-SC0002357.

Author contributions

D.C., A.K. and Y.S.M initiated the manuscript preparation. K.T., S.R., Z.W., R.V.D.L., S.P., H.Y., A.Y. and A.K. conceived cell architecture, optimized processing parameters and performed electrochemical testing at Ensurge Micropower. D.C., A.K. and Y.S.M co-wrote the manuscript. All the authors participated in the results discussion and commented on the manuscript.

Declaration of Interests

Y.S.M. is a member of the technical advisory board for Ensurge Micropower.

References

1. Rao, G. V. S. & Tsang, J. C. (1974) Electrolysis method of intercalation of layered transition metal dichalcogenides. *Mater. Res. Bull. 9*, 921–926.
2. Goodenough, J. B., Mizushima, K. & Wiseman, P. J. (1976) Electrochemical cell and method of making ion conductors for said cell. *UNITED KINGDOM ATOMIC ENERGY AUTHORITY* vol. 13 258–283.
3. Xu, K. (2014) Electrolytes and interphases in Li-ion batteries and beyond. *Chem. Rev. 114*, 11503–11618.
4. Tan, D. H. S., Banerjee, A., Chen, Z. & Meng, Y. S. (2020) From nanoscale interface characterization to sustainable energy storage using all-solid-state batteries. *Nat. Nanotechnol. 15*, 1–11.
5. Banerjee, A., Wang, X., Fang, C., Wu, E. A. & Meng, Y. S. (2020) Interfaces and Interphases in All-Solid-State Batteries with Inorganic Solid Electrolytes. *Chem. Rev. 120*, 6878–6933.
6. J.B. Bates, N.J. Dudney, G.R. Gruzalski, R.A. Zuhr, A. Choudhury, C. F. L. (1992) Electrical properties of amorphous lithium electrolyte thin films. *Solid State Ionics 29*, 42–44.
7. Bates, J. B., Dudney, N. J., Gruzalski, G. R., Zuhr, R. A., Choudhury, A., Luck, C. F. & Robertson, J. D. (1993) Fabrication and characterization of amorphous lithium electrolyte thin films and rechargeable thin-film batteries. *J. Power Sources 43*, 103–110.
8. Wang, Z., Santhanagopalan, D., Zhang, W., Wang, F., Xin, H. L., He, K., Li, J., Dudney, N. & Meng, Y. S. (2016) In situ STEM-EELS observation of nanoscale interfacial phenomena in all-solid-state batteries. *Nano Lett. 16*, 3760–3767.

9. Cheng, D., Wynn, T. A., Wang, X., Wang, S., Zhang, M., Shimizu, R., Bai, S., Nguyen, H., Fang, C., Kim, M., *et al.* (2020) Unveiling the Stable Nature of the Solid Electrolyte Interphase between Lithium Metal and Lipon Via Cryogenic Electron Microscopy. *Joule 4*, 2484–2500.

10. Dudney, N. J. (2005) Solid-state thin-film rechargeable batteries. *Mater. Sci. Eng. B Solid-State Mater. Adv. Technol. 116*, 245–249.

11. Li, J., Ma, C., Chi, M., Liang, C. & Dudney, N. J. (2015) Solid electrolyte: The key for high-voltage lithium batteries. *Adv. Energy Mater. 5*, 1–6.

12. Put, B., Mees, M. J., Hornsveld, N., Hollevoet, S., Sepúlveda, A., Vereecken, P. M., Kessels, W. M. M. & Creatore, M. (2019) Plasma-Assisted ALD of LiPO(N) for Solid State Batteries. *J. Electrochem. Soc. 166*, A1239–A1242.

13. Li, J., Dudney, N. J., Nanda, J. & Liang, C. (2014) Artificial solid electrolyte interphase to address the electrochemical degradation of silicon electrodes. *ACS Appl. Mater. Interfaces 6*, 10083–10088.

14. Santhanagopalan, D., Qian, D., McGilvray, T., Wang, Z., Wang, F., Camino, F., Graetz, J., Dudney, N. & Meng, Y. S. (2014) Interface limited lithium transport in solid-state batteries. *J. Phys. Chem. Lett. 5*, 298–303.

15. Neudecker, B. J., Dudney, N. J. & Bates, J. B. (2000) "Lithium-Free" Thin-Film Battery with In Situ Plated Li Anode. *J. Electrochem. Soc. 147*, 517.

16. Bates, J. B., Dudney, N. J., Gruzalski, G. R. & Luck, C. F. Thin Film Battery And Method For Making Same. *U.S.patent US 5,338,6*, 1994 Aug 16.

17. ST MICRO. (2014) EnFilm ™ - rechargeable solid state lithium thin film battery. *Online 30/10/2015*, 1–8.

18. Bhardwaj, R. C. Charging techniques for solid-state batteries in portable electronic devices. *U.S.patent US 9,553,4*, 2017 Jan 24.

19. ST MICRO. EFL700A39 EnFilm Rechargeable Battery - STMicro | DigiKey. https://www.digikey.com/en/product-highlight/s/stmicroelectronics/efl700a39-enfilm-rechargeable-battery.

20. cymbet. *EnerChip^{TM} CBC012 Features*. www.cymbet.com.

21. Muñoz, F., Durán, A., Pascual, L., Montagne, L., Revel, B. & Rodrigues, A. C. M. (2008) Increased electrical conductivity of LiPON glasses produced by ammonolysis. *Solid State Ionics 179*, 574–579.

22. Westover, A. S., Kercher, A. K., Kornbluth, M., Naguib, M., Palmer, M. J., Cullen, D. A. & Dudney, N. J. (2020) Plasma Synthesis of Spherical Crystalline and Amorphous Electrolyte Nanopowders for Solid-State Batteries. *ACS Appl. Mater. Interfaces 12*, 11570–11578.

23. López-Aranguren, P., Reynaud, M., Głuchowski, P., Bustinza, A., Galceran, M., López del Amo, J. M., Armand, M. & Casas-Cabanas, M. (2021) Crystalline LiPON as a Bulk-Type Solid Electrolyte. *ACS Energy Lett.* 445–450 doi:10.1021/acsenergylett.0c02336.

24. Tikekar, M. D., Choudhury, S., Tu, Z. & Archer, L. A. (2016) Design principles for electrolytes and interfaces for stable lithium-metal batteries. *Nature Energy* vol. 1 1–7.

25. Lin, D., Liu, Y. & Cui, Y. (2017) Reviving the lithium metal anode for high-energy batteries. *Nat. Nanotechnol. 12*, 194–206.

26. Han, X., Gong, Y., Fu, K., He, X., Hitz, G. T., Dai, J., Pearse, A., Liu, B., Wang, H., Rubloff, G., *et al.* (2017) Negating interfacial impedance in garnet-based solid-state Li metal batteries. *Nat. Mater. 16*, 572–579.

27. Han, F., Westover, A. S., Yue, J., Fan, X., Wang, F., Chi, M., Leonard, D. N., Dudney, N. J., Wang, H. & Wang, C. (2019) High electronic conductivity as the origin of lithium dendrite formation within solid electrolytes. *Nat. Energy* doi:10.1038/s41560-018-0312-z.

28. Yan, K., Lu, Z., Lee, H. W., Xiong, F., Hsu, P. C., Li, Y., Zhao, J., Chu, S. & Cui, Y. (2016) Selective deposition and stable encapsulation of lithium through heterogeneous seeded growth. *Nat. Energy 1*, 16010.

29. Liu, J., Bao, Z., Cui, Y., Dufek, E. J., Goodenough, J. B., Khalifah, P., Li, Q., Liaw, B. Y., Liu, P., Manthiram, A., *et al.* (2019) Pathways for practical high-energy long-cycling lithium metal batteries. *Nat. Energy* 10.1038/s41560-019-0338–x doi:10.1038/s41560-019-0338-x.

30. Zachman, M. J., Tu, Z., Choudhury, S., Archer, L. A. & Kourkoutis, L. F. (2018) Cryo-STEM mapping of solid–liquid interfaces and dendrites in lithium-metal batteries. *Nature 560*, 345–349.

31. Li, Y., Li, Y., Pei, A., Yan, K., Sun, Y., Wu, C. L., Joubert, L. M., Chin, R., Koh, A. L., Yu, Y., *et al.* (2017) Atomic structure of sensitive battery materials and interfaces revealed by cryo–electron microscopy. *Science (80-.). 358*, 506–510.

32. Fang, C., Li, J., Zhang, M., Zhang, Y., Yang, F., Lee, J. Z., Lee, M.-H., Alvarado, J., Schroeder, M. A., Yang, Y., *et al.* (2019) Quantifying inactive lithium in lithium metal batteries. *Nature 572*, 511–515.

33. Hood, Z. D., Chen, X., Sacci, R. L., Liu, X., Veith, G. M., Mo, Y., Niu, J., Dudney, N. J. & Chi, M. (2021) Elucidating Interfacial Stability between Lithium Metal Anode and Li Phosphorus Oxynitride via in Situ Electron Microscopy. *Nano Lett. 21*, 151–157.

34. Cheng, D., Wynn, T., Lu, B., Marple, M., Han, B., Shimizu, R., Sreenarayanan, B.,

Bickel, J., Hosemann, P., Yang, Y., *et al.* (2023) A free-standing lithium phosphorus oxynitride thin film electrolyte promotes uniformly dense lithium metal deposition with no external pressure. *Nat. Nanotechnol.* doi:10.1038/s41565-023-01478-0.

35. Oukassi, S., Salot, R., Bazin, A., Secouard, C., Chevalier, I., Poncet, S., Poulet, S., Boissel, J. M., Geffraye, F. & Brun, J. (2019) Millimeter scale thin film batteries for integrated high energy density storage. *Tech. Dig. - Int. Electron Devices Meet. IEDM 2019-Decem*, 618–621.

36. Wang, Z., Lee, J. Z., Xin, H. L., Han, L., Grillon, N., Guy-Bouyssou, D., Bouyssou, E., Proust, M. & Meng, Y. S. (2016) Effects of cathode electrolyte interfacial (CEI) layer on long term cycling of all-solid-state thin-film batteries. *J. Power Sources 324*, 342–348.

37. Wang, B., Bates, J. B., Hart, F. X., Sales, B. C., Zuhr, R. A. & Robertson, J. D. (1996) Characterization of Thin-Film Rechargeable Lithium Batteries with Lithium Cobalt Oxide Cathodes. *J. Electrochem. Soc. 143*, 3203.